Journal of Applied Microbiology, 0, 2022, lxac028

doi: 10.1093/jambio/lxac028
Advance Access Publication Date: 0 2022
Original Article

ORIGINAL ARTICLE

Geobacillus stearothermophilus and *Bacillus atrophaeus* spores exhibit linear inactivation kinetic performance when treated with an industrial scale vaporized hydrogen peroxide (VH_2O_2) sterilization process

Brian McEvoy[1,2], Ana Maksimovic[1,*] and Neil J Rowan[2]

[1]STERIS Applied Sterilization Technologies, IDA Business and Technology Park, Tullamore, Ireland and [2]Bioscience Research Institute, Technological University of the Shannon Midlands Midwest, Athlone Campus, Ireland

*Corresponding author. STERIS Applied Sterilization Technologies, IDA Business and Technology Park, Tullamore, Ireland. R35×865. Tel/Fax: +353852755825; E-mail: ana_maksimovic@steris.com

Keywords: Vaporized hydrogen peroxide sterilization; *Geobacillus*; bacterial endospores; terminal gaseous sterilization; medical devices; inactivation kinetics

Introduction

Many medical devices are supplied as sterile for safe patient care (McEvoy and Rowan 2019). The global sterilization services market is projected to reach USD 5.5 billion by 2026, growing at a compound annual growth rate (CAGR) of 6.0%, primarily driven by increasing surgical procedures, the prevalence of hospital-acquired infections and increased outsourcing of sterilization services (Anon 2021, McEvoy *et al*. 2021). A sterilization process may be defined as a "series of actions or operations needed to achieve the specified requirements for sterility" (ISO 2018). Sterility is not an absolute; therefore, it must be predicted and expressed in terms of the probability of achieving the inactivation of microbial and other infectious agents post-sterilization treatment (McEvoy and Rowan 2019). Moreover, the underpinning sterility assurance level (SAL) is defined as the 'probability of a single viable microorganism occurring on an item after sterilization' (ISO 2018). A sterilization process is validated whereby a pre-determined SAL is demonstrated through a series of process evaluations (McEvoy and Rowan 2019). In accordance with ISO14937:2009, microbicidal effectiveness must be established such that it is plausible to predict the probability of a defined resistant microorganism surviving exposure to a defined treatment.

In radiation processing, validation is performed through verification of the appropriateness of a delivered dose of sterilant to inactivate the microorganisms occurring on medical devices, where it is assumed that the commensurate microbial inactivation kinetics have been demonstrated as first order (Tallentire *et al*. 2010, Tallentire and Miller 2015, Hansen *et al*. 2020). Such first-order microbial inactivation has been demonstrated through the dose-related killing of *Bacillus pumilus* as a representative challenge microorganism. The best evidence indicates that nucleic acids are the main target of biocidal action for some sterilization modalities, such as radiation and ethylene oxide where first-order relationships can occur (Mosley 2003). Biological indicators (BIs) are employed to demonstrate microbicidal efficacy in gaseous and vapour sterilization processes such as ethylene oxide, steam, and vaporized hydrogen peroxide (VH_2O_2) processes. BIs are enclosed in process challenge devices (PCDs) during the validation of industrial sterilization modalities to provide sufficient resistance to the applied process (Shintani 2017).

With VH_2O_2 processing, a BI-containing *Geobacillus stearothermophilus* is selected and validated, due to its higher endospore

Received: 28 July 2022; **Revised:** 5 September 2022

resistance (D-value) compared to the bioburden that contaminates medical devices, which is carried out in accordance with ISO14937:2009 and ISO22441:2022. A D-value is defined as the exposure time to achieve a one-log reduction in the treated microbial population using a fixed dose of sterilant (McEvoy *et al*. 2021). Using what is typically an 'overkill' validation method in terms of the applied sterilant dose, a sterilization process is performed at 'half-cycle' parameters where full lethality of the treated BI is achieved that encompasses a minimum of 6-log reduction. Sterilant exposure is then doubled to achieve a theoretical 12 log reduction, where the additional 6-log reduction is extrapolated where it is assumed that inactivation follows first-order linear kinetics. Such a 12D process can be approximated based on an understanding of inactivation kinetics on a semi-logarithmic plot when the sterilizing conditions (i.e. process temperature, RH, and VH_2O_2 concentration) remain consistent for the duration of the exposure time (McEvoy and Rowan 2019). While, international sterilization standards such as ISO14937 require the establishment of the 'mathematical relationship defining the microbial inactivation', first-order log-linear microbial inactivation kinetics are often assumed to achieve predictability, allowing for the extrapolation to the desired SAL. Given the criticality of extrapolation to a desired SAL, the threshold for linearity, as determined by the coefficient of determination (R^2) of the survivor curve, should not be less than 0.8 (ISO 2019).

However, it has been previously demonstrated that first-order linear inactivation-type kinetic data may not be readily achieved, such as when microorganisms are exposed to relatively mild inactivation conditions that can stress-harden these microorganisms to subsequent lethal applied doses of the same or different processing stress, which can yield a low number of survivors (Rowan 1999, Rowan *et al*. 2007, Bradley *et al*. 2012, Garvey *et al*. 2015, Fitzhenry *et al*. 2019, Rowan 2019). Under such non-linear conditions that can be experienced using non-thermal food processing technologies, inactivation kinetic data curves can exhibit pronounced initial shoulders, extended tails, or sigmoid curves that are challenging to fit the primary data (Rowan *et al*. 2015). Non-linear inactivation has been previously reported for VH_2O_2 treatments, where the phenomenon of biphasic inactivation was described, which was being attributed to a number of potential sources including micro-condensation (Unger-Bimczok *et al*. 2008, Dufresne and Richards 2016), and the physiological factors associated with the treated BIs (Agalloco and Akers, 2013; Shintani 2014). However, the cellular and molecular mechanisms underpinning the VH_2O_2-mediated destruction of bacterial endospores remain to be fully understood (Linley *et al*. 2012, McEvoy and Rowan 2019).

Previous researchers have reported the use of chemical biocides that produced non-linear inactivation curves (Rowan *et al*. 2021) that were attributed to different theoretical models, namely, the 'vitalistic theory' that describes the phenotypic variation of microorganisms (Cerf 1977, Humpheson *et al*. 1998, Stone *et al*. 2009) and the 'mechanistic theory' that describes influencing factors that were associated with the applied sterilization process. The latter theory encompasses concepts such as superdormancy, biocide quenching, microorganism clumping, and biocidal action itself as possible contributing sources underpinning non-linear sterilization processing (Johnston *et al*. 2000, Lambert and Johnston 2000, Dhar and McKinney 2007, Shintani 2014).

Previous researchers have also reported on the use of predictive microbiology to address non-linear inactivation kinetic plots by applying various mathematical models that reflect the shape of different curves such as Weibull, Hom, and Gompertz (Lambert and Johnston 2000, Geeraerd *et al*. 2005, Coroller *et al*. 2006, Stone *et al*. 2009, Bevilacqua *et al*. 2015). Effective modeling of microbial inactivation arising from physical, chemical, or gaseous treatment modalities typically requires the plot to encompass a 6-log reduction in microbial count (or survival ratio) versus time data (Buzrul 2017). This is important as a dose-response curve is necessary to address the potential occurrence of microbial variance and possible resistance to the applied stress that may exhibit different inactivation shapes, which can be interpreted through a mathematical best-fit (Garre *et al*. 2020, Feurhuber *et al*. 2022). Additionally, numerous log reductions of treated BIs are required to effectively interpret and fit the inactivation plots (Rowan *et al*. 2015, Rowan 2019), which also supports international standardization of processes.

Thus, this constitutes the first detailed study to report on the inactivation kinetics of *G. stearothermophilus* spores that were subjected to VH_2O_2 treatment in an industrial sterilization process. Inactivation kinetic data for *Bacillus atrophaeus* were also determined using similar VH_2O_2 treatments to establish if first-order kinetics produced are specific to the treated microorganism. The impact of sterilant residues was elucidated to establish that the observed VH_2O_2-mediated inactivation was solely attributed to the sterilization process. In addition, scanning electron microscopy was employed to determine if a uniform monolayer of dispersed BI spores occurred during VH_2O_2 treatments where this occurrence provides additional insights into the potential impact of this sterilization process on treated endospore morphology.

Materials and methods

PCD preparation

PCDs were prepared by placing a BI of *G. stearothermophilus* (ATCC 12980) steel coupon (STERIS, Mentor, USA, Lot: AH-126) along with a Sterafirm VH2O2 chemical indicator (STERIS, Mentor, OH, USA,) into a 10 ml Luer lock syringe (Becton Dickinson, Franklin Lakes, NJ, USA) with a 15 cm flexible PVC lumen (3.5 mm internal diameter) attached. A PCD with a 15 cm lumen was determined to be an appropriate challenge following initial trials with lumens of various lengths (unpublished data). The syringe was sealed [150°C [+/−2°C], 40 psi [+/−5 psi] for 1 s] within a vented foil pouch (Nelipak, Ireland) (Fig. 1). Similarly, PCDs containing a BI of *B. atrophaeus* (ATCC 9372) steel coupon (MesaLabs, Bozeman, USA, Lot AG-022) were prepared by placing into a 10 ml luer lock syringe with varying lengths of flexible PVC lumen for PCD evaluation.

Inactivation of *Geobacillus stearothermophilus* PCDs with VH_2O_2

PCDs were fixed to the VH_2O_2 loading cart using Sellotape; thereafter, the cart was loaded to the industrial LTS-V VH_2O_2 sterilizer (STERIS, Mentor, USA) that had a chamber volume of 2025 l. VH_2O_2 processing was performed in the chamber supplied with 35% Vaprox sterilant (STERIS, Mentor, OH, USA). A standardized VH_2O_2 process consisting of the parameters of 35°C, minimum vacuum 4 millibars, and 5-pulse aeration was developed (Fig. 2). Sterilant concentration varied by injection of a fixed number of pulses (from one to a maximum of five pulses), each with approximately 5 mg l^{-1} VH_2O_2. Following processing, PCD samples were removed, and BI coupons were enumerated and

Figure 1 PCD comprising of a chemical and biological indicator placed into a 10 ml syringe with 15 cm lumen length (left), which is then sealed inside a SteriVent pouch with a Tyvek window (right).

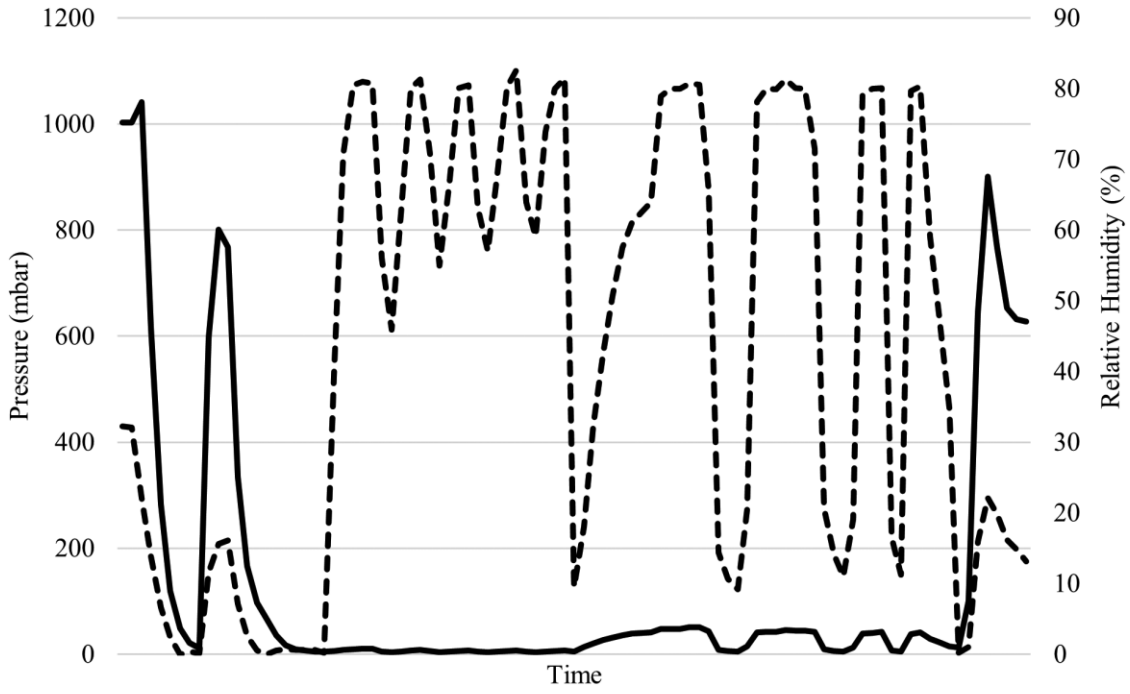

Figure 2 Schematic of the pressure and relative humidity (RH) profile of a 5-pulse VH_2O_2 process. Parameters: chamber pressure (—); chamber RH (—).

imaged by Scanning Electron Microscopy, while chemical indicators were visually examined for colour change. VH_2O_2 inactivation cycles were performed for both microorganism types and in triplicate for each survivor curve data point. To generate sufficient data points to meet a first survivor curve, 10 replicates (BIs) were used in each of the 1–5 pulse cycles. The number of replicates was reduced to 7 in the second and third VH_2O_2 processing runs.

Inactivation of *Bacillus atrophaeus* PCDs with VH_2O_2

PCDs of varying lumen lengths (15, 20, 25 cm) were trialled using varying combinations of sterilant pulses and survivor growth was enumerated to compare with kinetic inactivation data achieved using *G. stearothermophilus* PCDs. Thus, following the selection of an appropriate PCD, a survivor curve was generated by exposure to varying pulses of VH_2O_2 (1–5 pulses), in triplicate. A total of seven replicates (BIs) were used for each survivor curve data point. Representative samples during VH2O2 treatments were also recovered for imaging by SEM.

Enumeration of biological indicators

Geobacillus stearothermophilus enumeration

G. stearothermophilus BIs were aseptically removed from packaging and transferred into individual sterile glass test tubes containing 10 ml sterile purified water, which were then sonicated (Transsonic T890, Germany) for 25 min at 35 kHz. After sonication, 1:10 serial dilutions were prepared in sterile purified water. Selected dilutions were pour plated in duplicate in Tryptic soy agar (TSA; Biokar, France) cooled to approximately 45°C. Solidified plates were incubated inverted at 55–60° C for 48 h (48 h was determined in pre-study trials to be an appropriate incubation period for the BIs being tested following fractional treatment with VH_2O_2), after which plates were counted. For each treatment point, catalase was used to establish if any residual VH_2O_2 was absorbed onto the carrier to consider if this had any detrimental effect on spore viability, where studies were conducted in triplicate. Tubes of sterile dH_2O were replaced with Phosphate Buffer Saline (pH 7.1–7.5, Sigma Lifescience Ireland) containing 0.2 mg bovine liver catalase (2000–5000 units/mg protein; Sigma Aldrich, Germany) as similarly described by the method of Malik *et al.* 2013.

Bacillus atrophaeus enumeration

B. atrophaeus BI coupons (MesaLabs, Apex discs GRS-090) were aseptically removed from packaging and transferred into individual sterile glass test tubes containing 5 ml sterile Tween-80 (0.1%) and four 6 mm sterile glass beads. Tubes were sonicated for a minimum of 3 min at 35 kHz followed by vortexing for a minimum of 5 min. Then 5 ml of sterile purified water was added and tubes were vortexed for an additional 30 s. Thereafter, 1:10 serial dilutions were prepared in sterile purified water and selected dilutions were pour plated in duplicate in TSA (Biokar, France) cooled to approximately 40°C. Solidified plates were incubated at 30–35°C for 48 h, after which plates were counted.

Microbial inactivation kinetic data determination and statistical analysis and statistics

Microbial survivor curves were generated by plotting the logarithm of the survivor fraction ($\log_{10} N/N_o$) against the number of pulses of VH_2O_2 (or VH_2O_2 concentration); where N_o represents untreated spores and N represents the surviving fraction of VH_2O_2-treated spores. By using the ideal gas law ($pV = nRT$), VH_2O_2 concentration was calculated for each pulse. Survivor curves were generated separately for both BIs using triplicate VH_2O_2 processing runs. Microbial survivor curves were also generated for the treated *G. stearothermophilus*, where catalase was used to determine the impact of sterilant residue on spore inactivation. Regression analyses were performed and the average D-values were calculated from the slope of VH_2O_2-generated survivor plots (ISO 11138–7:2019) for each treated BI. Statistical analysis was conducted to determine the impact of VH_2O_2 residues on spore viability via Minitab software using *t*-testing at the 95% confidence level (alpha of 0.05).

Scanning electron microscopy

Non-destructive SEM EDX (Energy Dispersive X-ray) analysis was performed using a TESCAN SEM (Brno, Czech Rep.) with an EDX detector for elemental profiling set at 20 keV. Stainless steel BI specimens were mounted onto aluminium sample stubs coated with a surface adhesive to hold them in place. Images were obtained at 10 000× and 40 000× and examined for structural modification following treatment with VH_2O_2.

Results

Inactivation of *Geobacillus stearothermophilus* spores using VH_2O_2 treatments

Findings reveal that the spore populations of *G. stearothermophilus* were gradually decreased following treatments with 1–5 pulses of VH_2O_2, as shown in Fig. 3. The microbial inactivation plot follows a first-order linear kinetic shape where the R^2 coefficient was measured at 0.91. Moreover, the number of recovered BIs (n) has also declined with an increased number of applied VH_2O_2 pulses (Table 1). For example, all *G. stearothermophilus* BIs were recovered (96.83%) after 1-pulse cycle, while only 15.24% of BIs were recovered after a 5-pulse cycle.

The rapid inactivation of BI spores corresponds to the increasing sterilant concentration from zero to 1 pulse (Fig. 3). Subsequent examination of the pulse duration revealed that not all pulses were of equal duration or sterilant concentration. This is attributed to how the steriliser controls the process: as part of the preconditioning step prior to sterilant injection, relative humidity (RH) is reduced to a level of 0.0%–0.1% RH. In the first pulse, the sterilant is injected from this starting RH and a vacuum set-point of 4 millibar (mb) to a control endpoint of 80% RH. However, for all other pulses thereafter, vacuums are pulled to a set-point of 4 mb, but RH does not reduce to zero as there are no additional preconditioning steps. With each vacuum, RH reduces to a typical value of 46%–56% RH. Consequently, with an injection set-point of 80%, the injection on pulses after pulse 1 is less (delta injection of only 34%–24% RH), with less sterilant and less overall exposure time. Thus, when accounting for this variance in sterilant concentration by pulse, inactivation plotted against sterilant concentration revealed an improved linearity value of R^2=0.98 (Fig. 4). The appearance of chemical indicators is shown in Fig. 5, demonstrating VH_2O_2 penetration of the 15 cm lumen PCD after two pulses.

Effect of residual VH_2O_2 on the survivor curve

During the preparation of the initial VH_2O_2-mediated survivor curve for *G. stearothermophilus*, a second set of samples was enumerated with the incorporation of catalase as a sterilant

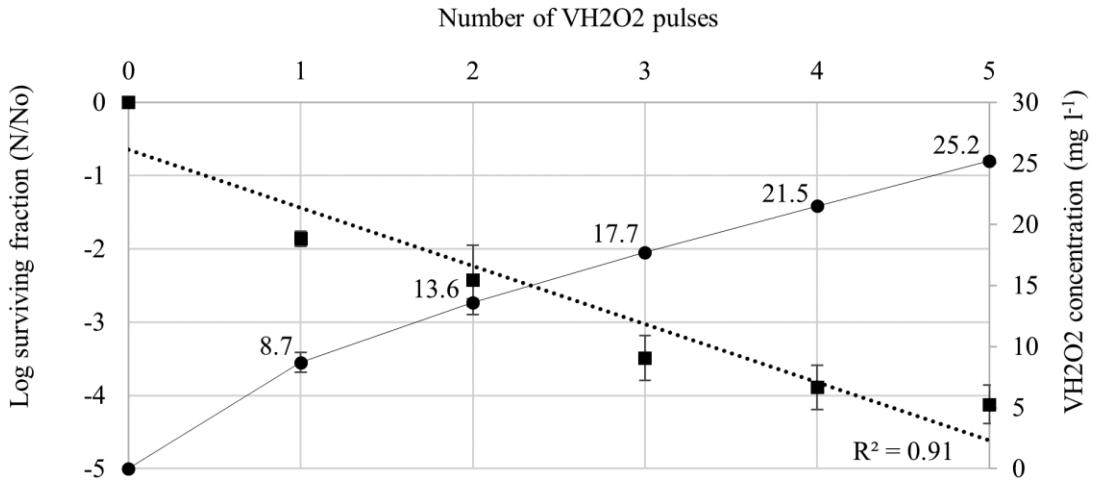

Figure 3 Survivor curve of *G. stearothermophilus* following treatment with pulses of VH_2O_2. *G. stearothermophilus* log surviving fraction in a 15 cm PCD (■) with vertical error bars showing standard deviation of N/N_o; calculated VH_2O_2 concentration (mg l^{-1}; •; values also shown) with error bars showing standard deviation of sterilant concentration; linear fit for *G. stearothermophilus* 15 cm PCD (•••).

Table 1 Percent recovery of *G. stearothermophilus* and *B. atrophaeus* BI spores following treatment with 1–5 pulses of VH_2O_2 sterilant.

Biological indicator	Number of pulses ± SD	Average exposure time (min)	Recovered biological indicators from triplicate runs (%)			
			Run 1	Run 2	Run3	Average
G. stearothermophilus	1	8.59 ± 0.49	100.00	100.00	90.48	96.83
	2	14.86 ± 0.66	90.00	100.00	82.38	90.79
	3	20.64 ± 0.36	70.00	100.00	90.00	86.67
	4	27.00 ± 0.50	30.00	71.43	38.57	46.67
	5	32.63 ± 0.70	20.00	14.29	11.43	15.24
B. atrophaeus	1	9.35 ± 1.01	100.00	100.00	57.14	85.71
	2	15.07 ± 1.22	100.00	100.00	100.00	100.00
	3	23.78 ± 1.29	42.86	42.86	42.86	42.86
	4	30.01 ± 2.18	42.86	57.14	71.43	57.14
	5	35.88 ± 2.53	85.71	28.57	14.29	42.86

Note: Pulses also expressed as average exposure time from triplicate runs.

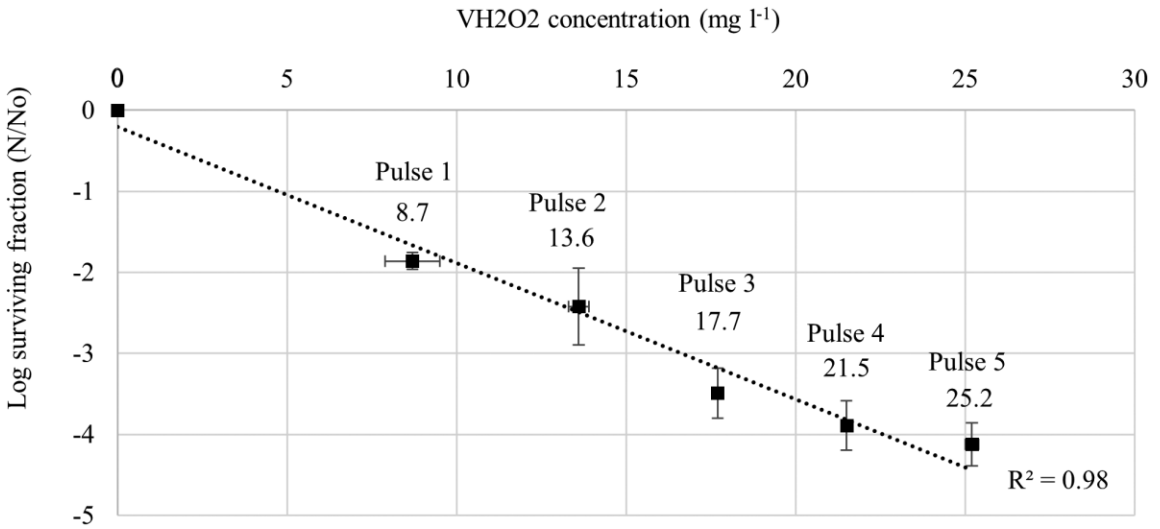

Figure 4 Survivor curve of *G. stearothermophilus* following treatment with incremental doses of VH_2O_2 sterilant. *G. stearothermophilus* log surviving fraction in a 15 cm PCD (■); linear fit for *G. stearothermophilus* 15 cm PCD (•••). Vertical error bars show standard deviation of N/N_o; horizontal error bars show standard deviation of sterilant concentration. Data labels show sterilant concentration (mg l^{-1}) and corresponding pulse number.

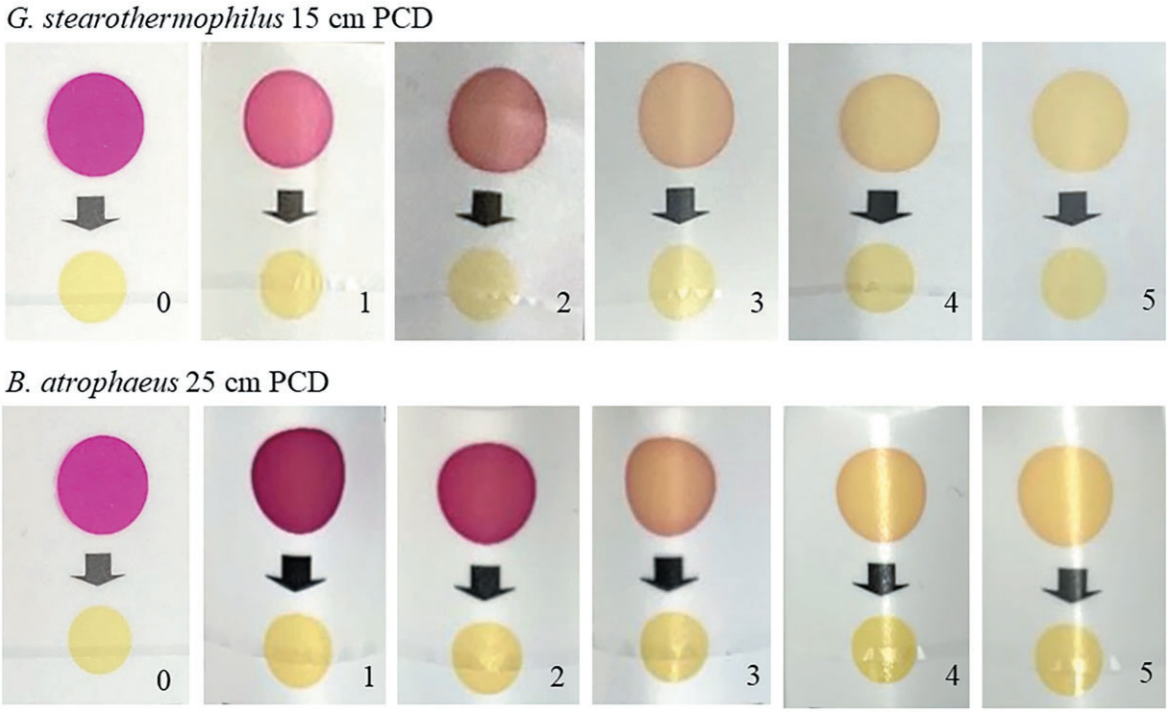

Figure 5 The appearance of untreated chemical indicator (0) and chemical indicators treated in 1, 2, 3, 4 and 5 pulse cycle. The labels 0–5 stand for the number of pulses used in the cycle. Chemical indicators used with *G. stearothermophilus* (top) were placed in the 15 cm PCD, while chemical indicators used with *B. atrophaeus* were placed in a 25 cm PCD (bottom).

quencher. Samples treated with catalase revealed that there was no statistical difference in these treatments ($P > .05$). It was noted that even if hydrogen peroxide had absorbed onto the BI carrier, this did not affect the VH_2O_2-treated spore viability.

Inactivation of *Bacillus atrophaeus* with VH_2O_2

Following the establishment of a microbial survivor plot using G. *stearothermophilus*, a range of PCDs containing *B. atrophaeus* were evaluated to find one appropriate for generating an appropriate measurable inactivation data plot over the required range of 1–5 pulses of VH_2O_2. The tested PCD types were as follows: syringe with 15, 20, 25, and 30 cm lumen length. First, all trialled PCDs were subjected to a 1-pulse cycle to establish the initial reduction in population and compared with the results obtained for *G. stearothermophilus* after 1-pulse cycle (Fig. 6). PCD with a lumen length of 30 cm was excluded from further analysis as it was deemed to be too technically challenging, whereas *B. atrophaeus* BIs in the shorter lumen length PCDs were enumerated following a 3-pulse cycle for lumen lengths of 15 and 20 cm, and a 4-pulse cycle for PCDs of 25 cm to determine their capacity to survive extensive VH_2O_2 treatment where these were compared with *G. stearothermophilus* data sets. As shown in Fig. 6, a PCD comprising of 25 cm lumen was found to closely match the established inactivation plot of G. *stearothermophilus*. Other lumen lengths were found to be either too challenging that required many pulses to achieve an inactivation plot over the 6-log regime or were deemed to be not sufficiently challenging as reflected in achieving inactivation after too few pulses to generate a clear microbial kinetic plot.

A survivor inactivation plot was generated using the PCD of 25 cm lumen with *B. atrophaeus*, (Fig. 7), where surviving BI fractions were plotted using the delivered sterilant concentration per pulse over the range of 1 to 5 pulses that were shown to exhibit $\log_{10}$ linear inactivation shape (R^2 coefficient, 0.93). The colour change of chemical indicators retrieved from this same VH_2O_2 process is shown in Fig. 5.

D-value calculations of *Geobacillus stearothermophilus* 15 cm PCD and *Bacillus atrophaeus* 25 cm PCD

D-values were calculated from the inverse of the slope of the survivor curve and summarized in Table 2.

SEM of *Geobacillus stearothermophilus* and *Bacillus atrophaeus* treated with VH_2O_2

SEM images of untreated, VH_2O_2 treated, and fully inactivated *G. stearothermophilus* and *B. atrophaeus* spores are shown in Fig. 8.

Upon visual observation of SEM images of the untreated and VH_2O_2-treated BIs, a well-distributed monolayer of spores was evident with no apparent change to the level of clumping or aggregation with regard to the inactivation process (the number of H_2O_2 pulses applied) (Fig. 9). Similar observations were made from SEM images of *B. atrophaeus* BIs treated with fractional and sterilization doses of vaporized hydrogen peroxide (VHP) and ethylene oxide gas (unpublished data).

Discussion

Following the establishment of an appropriate PCD and VH_2O_2 process, experimental studies were found to be very repeatable and were appropriate for producing a survivor plot of kinetic inactivation range using one to five pulses of VH_2O_2. As shown in Fig. 3, a first-order log-linear inactivation was observed for

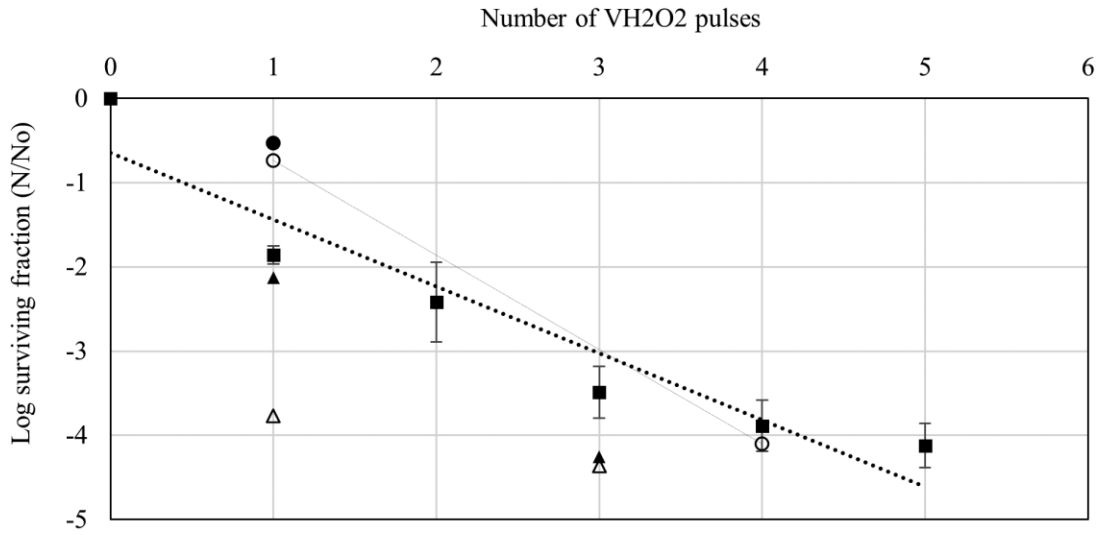

Figure 6 Survivor inactivation plots of PCDs containing *B. atrophaeus* that were compared with similarly treated *G. stearothermophilus* spore populations. A range of PCDs containing pre-determined numbers of *B. atrophaeus* spores with different degrees of resistance (15, 20, 25, and 30 cm lumen) were trialled to establish a PCD with a level of resistance comparable to *G. stearothermophilus*. As shown on the figure: *G. stearothermophilus*, 15 cm PCD (■); *B. atrophaeus*, 15 cm PCD (△); *B. atrophaeus*, 20 cm PCD (▲); *B. atrophaeus*, 25 cm PCD (■); *B. atrophaeus*, 30 cm PCD (●); linear fit *G. stearothermophilus*, 15 cm PCD (●●●); linear fit *B. atrophaeus*, 25 cm PCD (—).

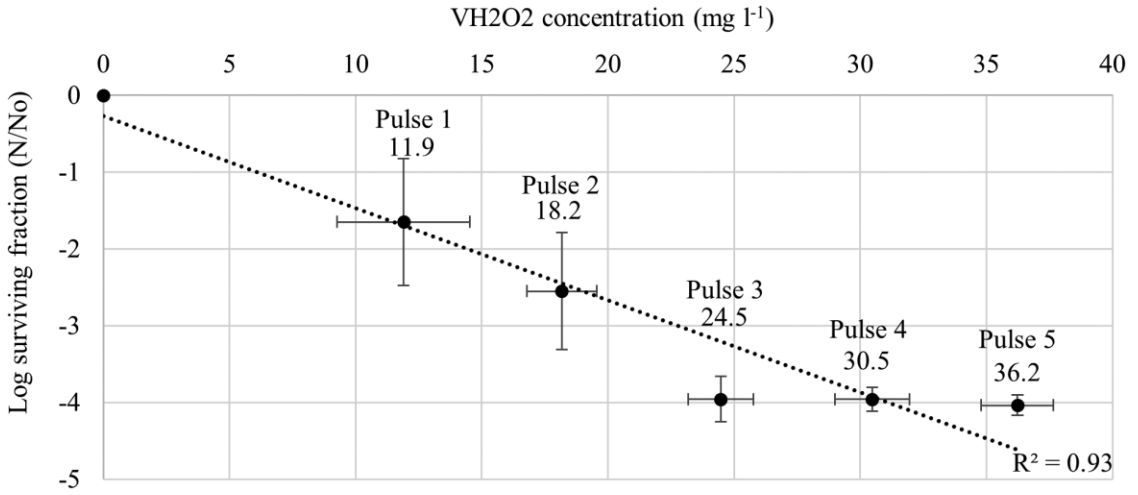

Figure 7 Survivor inactivation plot of *B. atrophaeus* following treatment with VH_2O_2 with increasing sterilant concentration. *B. atrophaeus* log surviving fraction in a 25 cm PCD (●); linear fit for *B. atrophaeus* in a 25 cm PCD (●●●). Vertical error bars show standard deviation of N/N_o; horizontal error bars show standard deviation contact time ($n = 3$). Data labels show sterilant concentration.

Table 2 Comparison of D-values and sterilization processing requirements, pulses of VH_2O_2 required for processing of PCDs containing *G. stearothermophilus* and *B. atrophaeus*.

Sterilization processing requirements	*G. stearothermophilus*	*B. atrophaeus*
BI D-value (min) (Manufacturer claim)	1.4	0.3
PCD	15 cm lumen	25 cm lumen
D-value (min)	7.75	8.72
12 SLR (Routine process time required for sterilization) (min)	93	104.64
Average pulse time from survivor curve (min)	7.24	7.90
VH_2O_2 Sterilization Process (Pulses of sterilant)*	13	14

*VH_2O_2 pulses are calculated based on 12 SLR time/average pulse time. Fractions of pulses are positively rounded to full integers.

the BI, *G. stearothermophilus* contained in a PCD comprising of a 10 ml syringe with a 15 cm lumen attached that was contained in a vented pouch. In compliance with ISO11138-7:2019, an R^2 coefficient of determination greater than 0.8 was achieved. Further examination of the duration and concentration of sterilant delivered in each VH_2O_2 pulse revealed that not all pulses were equal in these properties; therefore, the survivor inactivation

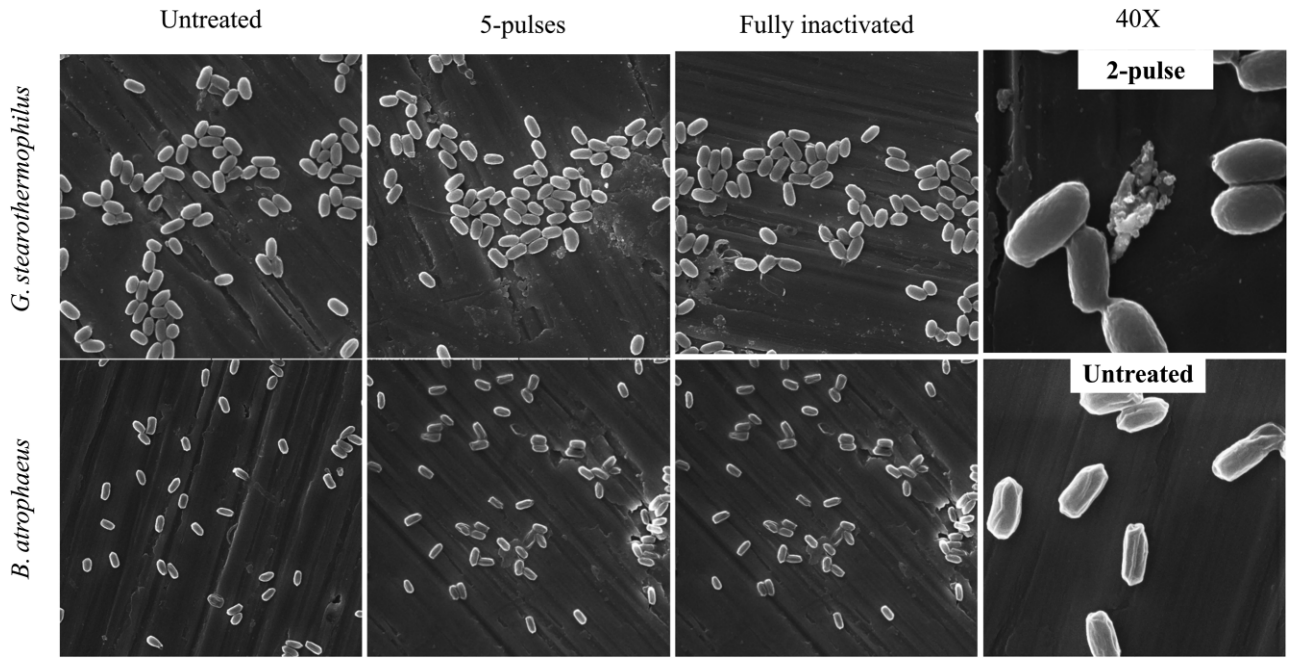

Figure 8 SEM images (10k×) of untreated *B. atrophaeus* and *G. stearothermophilus*, treated with five pulses and fully inactivated with VH_2O_2. Higher magnification (40k×) also shown of selected samples.

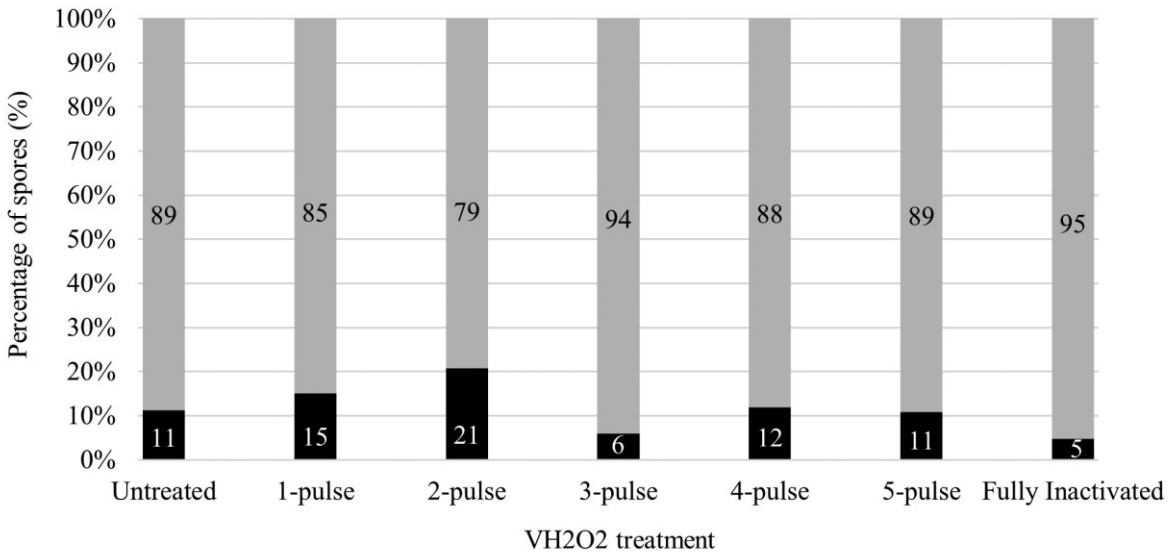

Figure 9 Count of *G. stearothermophilus* single spores (■) and grouped spores (≥ 2; ▨) from SEM images (10 000×). Data are provided for untreated spores, fully inactivated spores, and spores treated in VH_2O_2 cycles ranging from one to five pulses.

data were re-plotted to log survivor versus sterilant concentration that resulted in an improvement in R^2 of 0.98 (Fig. 4). This demonstrates the importance of establishing the most appropriate measure of 'sterilant dose' when assessing inactivation. In this work, pulses are not equal due to how the process is controlled by the sterilizer with the inactivation of the spores being a consequence of sterilant concentration and exposure time, which is potentially under-appreciated in the field of sterilization microbiology (McEvoy and Rowan 2019). The novel finding of the degree of linearity of the inactivation applies to industrial-scale sterilization with VH_2O_2 and demonstrates the appropriateness of the use of validation methods such as half-cycle overkill as described in ISO14937:2009. The D-value for VH_2O_2 sterilant exposure time of 7.75 min (SD = 0.40) was calculated to deliver 12 spore log reductions (or 12D), which is equivalent to a SAL of 10^{-6} in 93.00 min. With an average exposure time per pulse of 7.24 min, this equates to a routine sterilization process of 12.85 pulses. Similarly, D-value may be calculated in terms of sterilant concentration (M = 5.84 mg l^{-1}; SD = 0.22), and with an average concentration per pulse of 5.78 mg l^{-1}, determined to require a process of 12.12 pulses. Thus, to provide a SAL of 10^{-6} to the described PCD a routine process of 13 pulses must be programmed on the sterilizer. Furthermore, the demonstration of linearity also confirms that fractional methods

of D-value determination such as Holcomb–Spearman–Karber Procedure, Limited Holcomb–Spearman–Karber Procedure, and Stumbo–Murphy–Cochran Procedure may be applied (ISO 2019).

A range of PCDs was evaluated for *B. atrophaeus* by interpreting the linked survivor kinetic data generated from VH_2O_2-treated *G. stearothermophilus* in this study (Fig. 6). Given the lower D-value of the *B. atrophaeus* BI (D-value = 0.3 minutes) versus *G. stearothermophilus* BI (D-value = 1.4 min), a more challenging PCD was selected for survivor kinetic data plot generation: following treatment with one and four pulses of VH_2O_2, a 25 cm lumen PCD containing *B. atrophaeus* was found to yield a similar inactivation as the 15 cm PCD containing *G. stearothermophilus*. A survivor curve was constructed yielding an R^2 value of 0.93, in compliance of the requirements of ISO11138-7:2019.

The type of sterilization process and associated experimental conditions are significant factors that inform the reliable and repeatable linear destruction of BIs over a period of approximately 45 min in industrial-scale sterilization using PCDs. This contrasts with previously reported studies where biphasic microbial inactivation kinetic plots were observed over much shorter durations of treatments such as within less than 5 min (Dufresne and Richards 2016). It is plausible that if the zero to one pulse range of this study was more closely examined in a BI evaluation resistometer (BIER) in the absence of a PCD, non-linear inactivation may potentially be observed: this is due to the inactivation kinetics being significantly shortened when the resistance of the PCD is removed and D-values more aligned to the BI manufacturer stated values, e.g., 1.4 min for *G. stearothermophilus* BI used in this study. In contrast, this present study has been performed in an industrial sterilizer with PCDs that are typically used to increase the microbiological challenge in the validation of such a sterilization process in accordance with the relevant ISO14937 standard.

As described by Shintani *et al.* (2010) and Shintani (2014), experimental artefact of spore clumping has been described as a potential source of non-linear inactivation kinetics, whereby the aggregation of spores result in reduced penetration of the sterilant vapour. Furthermore, the work of Johnston *et al.* (2000) demonstrated the significance of microbial load and the possibility for biocide quenching by the inoculum: as quenching occurs, the amount of available biocide for further inactivation of the population reduces at a microbial cellular level, thus resulting in the appearance of a more resistant sub-population of treated BIs. This was also evident for pulsed-plasma gas-discharge treated microbial samples that contained short-lived oxygenated free radicals (Rowan *et al.* 2007; Hayes *et al.* 2013). SEM may be effectively used as an investigative tool to provide visual data on the effect of sterilization processes on spore shape and surface topography; e.g. this was demonstrated for *Mycobacterium paratuberculosis* cells by pulsed electric field treatments (Rowan *et al.* 2001) and for *Campylobacter jejuni* cells treated with pulsed-plasma gas-discharge exposures (Rowan *et al.* 2008). In this work, the analysis of SEM images revealed (i) an evenly distributed monolayer of spores in treated and untreated BIs and (ii) no significant change to the distribution of spores on the BI carrier material either before or after treatment (Figs. 8 and 9). This is consistent with the findings of others who examined treatment with VHP and ethylene oxide (EO) sterilant and noticed no noticeable morphology differences or clumping of cells (Reich and Akkus 2013). Furthermore, the inclusion of catalase in the test method confirmed the absence of any observed sterilant residual effect on spore enumeration.

The appropriateness of *B. atrophaeus* as a potential BI system for use in VH_2O_2 is demonstrated in the survivor plot with rapid inactivation from one to three pulses of *B. atrophaeus* (Fig. 7). While the cycles in which *B. atrophaeus* were treated had somewhat higher VH_2O_2 concentration (Fig. 7) in the chamber, it is important to note that VH_2O_2 concentration in the chamber does not necessarily correspond to the VH_2O_2 concentration within the PCD. This was evident in the colour change in the chemical indicators: unlike *G. stearothermophilus*, no colour change was observed in the *B. atrophaeus* PCDs after two pulses (Fig. 5). This would indicate that the longer 25 cm lumen was effective in impeding the ingress of vapour. However, once vapour penetrated the PCD lumen, inactivation of the *B. atrophaeus* BI was rapid due to its lower intrinsic resistance, with a D-value of only 0.3 min as compared to *G. stearothermophilus* of 1.4 min (Table 2). This may also explain why spore inactivation is observed with 1- and 2- pulses of VH_2O_2 treatment even though limited penetration with sterilant. Thus, while the overall resistance of a PCD is a combination of the BI resistance and the PCD materials, the contribution of each constituent component may require some consideration when assessing both D-value and linearity.

Calculation of D-value for the *B. atrophaeus* PCD yielded a conservative figure of 8.72 min or 14 pulses for a routine sterilization process yielding SAL of 10^{-6}. If only pulses 1–3 were considered in the calculation of the slope of the line, then D-value would adjust to 6.07 min and 10 pulses. Thus, this demonstrates that experimental limitations conservatively add to the final process being delivered such that in this case it is likely that approximately four additional logs of kill are being delivered to the process, resulting in a SAL of 10^{-10}.

Furthermore, as shown by this research, the use of a 'most resistant organism', in this case *G. stearothermophilus*, does not seem to be the most important factor as it is the overall resistance of the PCD relative to the medical device being sterilized, which is of most importance when quantifying D-values and extrapolating to a required SAL. In this research, by modifying the lumen length of the PCD, similar D-values were obtained using two different biological indicator species. Hence, it may be argued that the criteria for an appropriate BI for use in industrial sterilization are one of (i) known high resistance within a PCD, (ii) known inactivation kinetics and linearity of the PCD, and (iii) one that may be qualified as equivalent or greater resistance relative to the natural microbiological challenge of the medical device itself. The generation of critical data points for VH_2O_2 sterilization will also inform the future automation of this process including the uses of digital technologies such as artificial intelligence enabled by machine learning (Rowan *et al.* 2022).

In conclusion, this constitutes the first study to examine the inactivation of two types of BI spores contained in PCDs and processed with an industrial VH_2O_2 sterilizer. Findings supported the occurrence of linear BI inactivation plots post-VH202 treatments, which is important given that validation methods underpinning terminal medical device sterilization rely upon this linear microbial death-rate assumption. Thus, this study provides additional rigour and confidence that an appropriate sterility level can be achieved using biological indicators using standard validation methods as described in the recently published ISO22441 standard for sterilization with VH_2O_2. Hence, this work furthers the advancement of VH_2O_2 for the terminal sterilization of medical devices that is critical for patient care.

Acknowledgements

The authors would like to acknowledge the team at STERIS who assisted with VH_2O_2 sterilization processing. For the support with SEM analysis, the authors would like to thank Dr.

Emer O'Neill and Dr. Alan Murphy of TUS. The authors acknowledge the Technological University of the Shannon Midlands Midwest Doctoral Scholarship Programme and funding support from STERIS AST.

References

Agalloco JP, Akers JE. Overcoming limitations of vaporized hydrogen peroxide: hydrogen peroxide is highly potent and highly problematic. *Pharm Technol* 2013;**9**:46–56.

Anon. Sterilization services market by method (ETO, gamma, steam, X-ray), type (contract sterilization, validation services), mode of delivery (off-site, on-site), end user (Hospitals and clinics, pharmaceuticals) - Global Forecasts (2022 - 2026). *Markets and Markets* 2021. https://www.marketsandmarkets.com/Market-Reports/sterilization-service-market-183597324.html?gclid=EAIaIQobChMI_6ifsb2H-AIVgQCLCh1jCw2OEAAYASAAEgK6DPD_BwE (30 May 2022, date last accessed).

Bevilacqua A, Speranza B, Sinigaglia M *et al.* A focus on the death kinetics in predictive microbiology: benefits and limits of the most important models and some tools dealing with their application in foods. *Foods* 2015;**4**:565–80.

Bradley D, McNeill B, Laffey JG *et al.* Studies on the pathogenesis and survival of different culture forms of listeria monocytogenes to pulsed UV-light irradiation after exposure to mild-food processing stresses. *Food Microbiol* 2012;**30**:330–9.

Buzrul S. Evaluation of different dose-response models for high hydrostatic pressure inactivation of microorganisms. *Foods* 2017;**79**:1–15.

Cerf O. Tailing of survival curves of bacterial spores. *J Appl Bacteriol* 1977;**42**:1–19.

Coroller L, Leguerinel I, Mettler E *et al.* General model, based on two mixed weibull distributions of bacterial resistance, for describing various shapes of inactivation curves. *Appl Environ Microbiol* 2006;**72**:6493–502.

Dhar N, McKinney JD. Microbial phenotypic heterogeneity and antibiotic tolerance. *Curr Opin Microbiol* 2007;**10**:30–38.

Dufresne S, Richards T. The first duel-sterilant low-temperature sterilization system. *Can J Infect Control* 2016;**3**:169–74.

Feurhuber M, Neuschwander R, Taupitz T *et al.* Mathematically modelling the inactivation kinetics of *Geobacillus stearothermophilus* spores: effects of sterilization environments and temperature profiles. *Phys Med* 2022;**13**:p.100046.

Fitzhenry K, Rowan N, de Rio AV *et al.* Inactivation efficacy of Bacillus endospores via modified flow-through PUV treatment with comparison to conventional LPUV treatment. *J Water Process Eng* 2019;**27**:67–76.

Garre A, Zwietering MH, den Besten HMW. Multilevel modelling as a tool to include variability and uncertainty in quantitative microbiology and risk assessment. Thermal inactivation of listeria monocytogenes as proof of concept. *Food Res Int* 2020;**137**:1–13.

Garvey M, Rabbity D, Stocca A *et al.* Pulsed light inactivation of *Pseudomonas aeruginosa* and *Staphylococcus aureus*. *Water Environment J* 2015;**29**:36–42.

Geeraerd AH, Valdramidis VP, van Impe JF. GInaFiT, a freeware tool to assess non-log-linear microbial survivor curves. *Int J Food Microbiol* 2005;**102**:95–105.

Hansen JM, Fidopiastis N, Bryans T *et al.* Radiation sterilization: dose is dose. *Biomed Instrum Technol* 2020;**54**:45–52.

Hayes J, Kirf D, Garvey M, Rowan NJ. Disinfection and toxicological assessments of pulsed UV and pulsed-plasma gas-discharge treated-water containing the waterborne protozoan enteroparasite *Cryptosporidium parvum*. *J Microbiol Methods* 2013;**94**:325–37.

Humpheson L, Adams MR, Anderson WA *et al.* Biphasic thermal inactivation kinetics in *Salmonella enteritidis* PT4. *Appl Environ Microbiol* 1998;**64**:459–64.

International Organization for Standardization (ISO). ISO22441:2022. *Sterilization of health care products—low temperature vaporized hydrogen peroxide—requirements for the development, validation and routine control of a sterilization process for medical devices*. Geneva: ISO, 2022.

International Organization for Standardization (ISO). ISO11138-7:2019. *Sterilization of health care products—biological indicators—Part 7: Guidance for the selection, use and interpretation of results*. Geneva: ISO, 2019.

International Organization for Standardization (ISO). ISO11139:2018. *Sterilization of health care products—vocabulary of terms used in sterilization and related equipment and process standards*. Geneva: ISO, 2018.

International Organization for Standardization (ISO). ISO14937:2009. *Sterilization of health care products—general requirements for characterization of a sterilizing agent and the development, validation and routine control of a sterilization process for medical devices*. Geneva: ISO, 2009.

Johnston MD, Simons EA, Lambert RJW. One explanation for the variability of the bacterial suspension test. *J Appl Microbiol* 2000;**88**:237–42.

Lambert RJW, Johnston MD. Disinfection kinetics: a new hypothesis and model for the tailing of log-survivor/time curves. *J Appl Microbiol* 2000;**88**:907–13.

Linley E, Denyer SP, McDonnell G *et al.* Use of hydrogen peroxide as a biocide: new consideration of its mechanisms of biocidal action. *J Antimicrob Chemother* 2012;**67**:1589–96.

McEvoy B, Lynch M, Rowan NJ. Opportunities for the application of real-time bacterial cell analysis using flow cytometry for the advancement of sterilization microbiology. *J Appl Microbiol* 2021;**130**:1794–812.

Malik DJ, Shaw CM, Rielly CD *et al.* The inactivation of *Bacillus subtilis* spores at low concentrations of hydrogen peroxide vapour. *J Food Eng* 2013;**114**:391–6.

McEvoy B, Rowan NJ. Terminal sterilization of medical devices using vaporized hydrogen peroxide: a review of current methods and emerging opportunities. *J Appl Microbiol* 2019;**127**:1403–20.

Mosley GA. Microbial lethality: when it is log-linear and when it is not. *Biomed Instrum Technol* 2003;**37**:451–3.

Reich MS, Akkus O. Sporicidal efficacy of genipin: a potential theoretical alternative for biomaterial and tissue graft sterilization. *Cell Tissue Bank* 2013;**14**:381–93.

Rowan NJ, Espiec S, Harrower J *et al.* Evidence of lethal and sublethal injury in food-bonre bacterial pathogens exposed to high-intensity pulsed-plasma gas-discharges. *Lett Appl Mirobiol* 2008;**46**:80–86.

Rowan NJ, Valdramidis VP, Gomez-Lopez VM. A review of quantitative methods to describe efficacy of pulsed light generated inactivation data that embraces the occurrence of viable but non culturable state microorganisms. *Trends Food Sci Technol* 2015;**44**:79–92.

Rowan NJ. Pulsed light as an emerging technology to cause disruption for food and adjacent industries—quo vadis? *Trends Food Sci Technol* 2019;**88**:316–32.

Rowan NJ, MacGregor SJ, Anderson JG *et al*. Inactivaion of *Mycobacterium paratuberculosis* by pulsed electric fields. *Appl Environ Microbiol* 2001;**67**:2833–6.

Rowan NJ, Espie S, Harrower J *et al*. Pulsed plasma gas discharge inactivation of microbial pathogens in chilled poultry wash water. *J Food Prot* 2007;**70**:2805–10.

Rowan NJ. Evidence that inimical food-preservation barriers alter microbial resistance, cell morphology and virulence. *Trends Food Sci Technol* 1999;**10**:261–70.

Rowan NJ, Meade E, Garvey M. Efficacy of frontline chemical biocides and disinfection approaches for inactivating SARS-CoV-2 variants of concern that cause coronovirus disease with the emergence of opportunities for green eco-solutions. *Curr Opin Environ Sci Health* 2021;**23**:1–13.

Rowan NJ, Murray N, Qiao Y *et al*. Digital transformation of peatland eco-innovations ('Paludiculture'): enabling a paradigm shift towards the real-time sustainable production of 'green-friendly' products and services. *Sci Total Environ* 2022;**3**:1–20.

Shintani H, Sakudo A, Burke P *et al*. Gas plasma sterilization of microorganisms and mechanisms of action. *Exp Ther Med* 2010;**1**:731–8.

Shintani H. Important points to attain reproducible sterility assurance. *Biochem Physiol* 2014;**03**:135.

Shintani H. Ethylene oxide gas sterilization of medical devices. *Biocontrol Sci* 2017;**22**:1–16.

Stone G, Chapman B, Lovell D. Development of a log-quadratic model to describe microbial inactivation, illustrated by thermal inactivation of *Clostridium botulinum*. *Appl Environ Microbiol* 2009;**75**:6998–7005.

Tallentire A, Miller A. Microbicidal effectiveness of X-rays used for sterilization purposes. *Radiat Phys Chem* 2015;**107**:28–130.

Tallentire A, Miller A, Helt-Hansen J. a comparison of the microbicidal effectiveness of gamma rays and high and low energy electron radiations. *Radiat Phys Chem* 2010;**79**:701–4.

Unger-Bimczok B, Kottke V, Hertel C, Rauschnabel **3**, 123-133. The influence of humidity, hydrogen peroxide concentration, and condensation on the inactivation of *Geobacillus stearothermophilus* spores with hydrogen peroxide vapor. *J Pharm Innov* 2008;**3**:123–33.